Supporting Information

Poruchynsky et al. 10.1073/pnas.1416418112

SI Materials and Methods

Protein Analysis in Nuclear and Cytoplasmic Fractions. Aliquots of whole-cell lysates or 10% of the volume of nuclear (N) or cytoplasmic (C) fractions were separated by SDS/PAGE. Blots were incubated in antibodies: ATM (mouse clone 2C1) and Histone H3 (goat), each from Santa Cruz; 53BP1 (rabbit, Novus); DNA-PK (mouse clone 18) and p53 (mouse Ab-6 clone DO-1), each from Calbiochem; ATR (rabbit), Rad50 (rabbit), Mre11 (rabbit), p95NBS1 (rabbit), and VDAC (rabbit), each from Cell Signaling; H2AX (rabbit antiserum, anti-histone H2AX), γ-H2AX (mouse monoclonal anti phospho-histone H2AX), and GAPDH (mouse monoclonal) each from Millipore; tubulin (DM1A, Sigma); poly (ADP-ribose) polymerase (PARP; rabbit polyclonal, Upstate); dynein (mouse clone IC74, Covance); or Bim (mouse C34C5, Cell Signaling).

Immunofluorescence. Fixed cells were incubated 45 min at 22 °C in 20% serum in PBS before incubation in the DNA repair protein primary antibody (DNA-PK, rabbit monoclonal clone Y393, Millipore; p95NBS1, rabbit monoclonal; and Mre11, rabbit polyclonal, each from Abcam; 53BP1, affinity-purified rabbit sera, Novus; p53, or Ab-7 sheep polyclonal, Calbiochem) for either 1 h at 22 °C or overnight at 4 °C, followed by washes in 5% (vol/vol) serum in PBS, secondary antibody conjugated to Rhodamine (Jackson Immunochemicals), followed by either α-tubulin (mouse monoclonal Clone DM1A, Sigma) or αβ-tubulin (rabbit, Cell Signaling) and the next secondary antibody conjugated to FITC. An antibody to gelsolin (mouse, Sigma-Aldrich) was used as a non-MT trafficking control. Other antibody controls, DAPI counterstaining for nuclei, and confocal microscopy imaging were as described previously (1, 2).

Dynein Immunoprecipitation. Mre11 and p53 immunoprecipitations were carried out as previously described for dynein. ATM immunoprecipitations were modified to Pierce Protein LPlus Agarose (Thermo Scientific) because of differences in the antibody class binding specificities. Unbound samples were collected after antibody-antigen bead incubation and before washing, and analyzed for protein concentration.

Proteomics. Cell lysate was immunoprecipitated with anti-dynein conjugated to M-270 Epoxy Dynabeads (Life Technologies). The enriched proteins were resolved by 4–15% SDS/PAGE gel. Lanes containing anti-dynein interacting proteins were cut into 20 segments. Each segment was digested with trypsin and analyzed by LC-MS/MS. Digested peptides were resuspended in 10 μL 0.1% formic acid and then analyzed on an LTQ-Orbitrap Elite (Thermo Scientific) and SilicaTip emitter (New Objective) for electrospray ionization. An Easy-nLC 1000 (Thermo Scientific) was used for on-line RPLC separation. The digested peptides were loaded onto a nano-trap column (Acclaim PepMap100 Nano Trap Column, C18, 5 μm, 100 Å, 100 μm i.d. × 2 cm) and separated on a nano-LC column (Acclaim PepMap100, C18, 3 μm, 100 Å, 75 μm i.d. × 25 cm, nanoViper). Mobile phases A and B consisted of 0.1% formic acid in water and 0.1% formic acid in 90% ACN, respectively. Peptides were eluted from the column at 250 nL/min using the following linear gradient: from 2 to 8% B in 5 min, from 8 to 32% B in 100 min, from 32 to 100% B in 10 min, and held at 100% B for an additional 10 min. The spray voltage was 2.2 kV. Full spectra were collected from m/z 350–1,800 in the Orbitrap analyzer at a resolution of 120,000, followed by data-dependent HCD MS/MS scans of the top 10 most-abundant ions, using 32% collision energy. A dynamic exclusion time of 30 s was used to discriminate against the previously analyzed ions.

Peptides and proteins were identified and quantified using the Maxquant software package (v1.3.0.5) with the Andromeda search engine as well as proteome discoverer with Mascot and Sequest search engines (Thermo Scientific). MS/MS spectra were searched against the Uniprot human protein database. The parameters used for data analysis include trypsin as a protease with two missed cleavage allowed. Carbamidomethyl cysteine was specified as a fixed modification. Deamidation of asparagine and glutamine, oxidation of methionine, and protein N-terminal acetylation were specified as variable modifications. The precursor mass tolerance was set to 7 ppm and fragment mass tolerance to 20 ppm. False-discovery rate was calculated using a decoy database and a 1% cut-off was applied.

1. Huff LM, Sackett DL, Poruchynsky MS, Fojo T (2010) Microtubule-disrupting chemotherapeutics result in enhanced proteasome-mediated degradation and disappearance of tubulin in neural cells. *Cancer Res* 70(14):5870–5879.

2. Poruchynsky MS, et al. (2008) Proteasome inhibitors increase tubulin polymerization and stabilization in tissue culture cells: A possible mechanism contributing to peripheral neuropathy and cellular toxicity following proteasome inhibition. *Cell Cycle* 7(7):940–949.

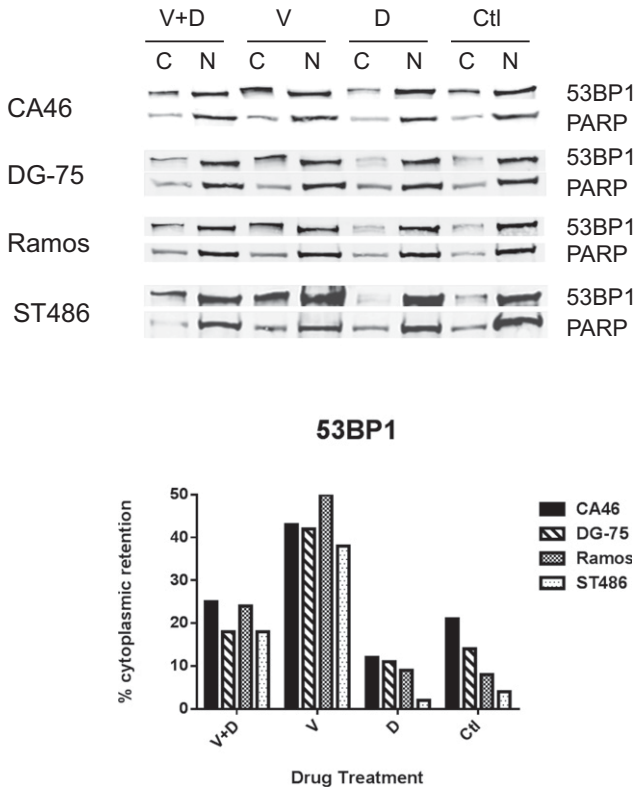

Fig. S1. Treatment of Burkitt's lymphoma cells with a MTA causes increased cytoplasmic retention of the DNA damage-repair protein 53BP1. Burkitt's lymphoma cell lines CA46, DG-75, Ramos, and ST486 were untreated (Ctl) or treated either with 100 nM vincristine (V) for 6 h, 400 ng/mL doxorubicin (D) for 4 h, or pretreated with 100 nM vincristine for 2 h before a combination treatment of both V plus D for another 4 h (V+D). Cytoplasmic (C) and nuclear (N) fractions of cell lysates are indicated for Western blots probed with antibodies for both 53BP1 and PARP. The percent cytoplasmic retention is calculated as $[C/(C+N)] \times 100\%$.

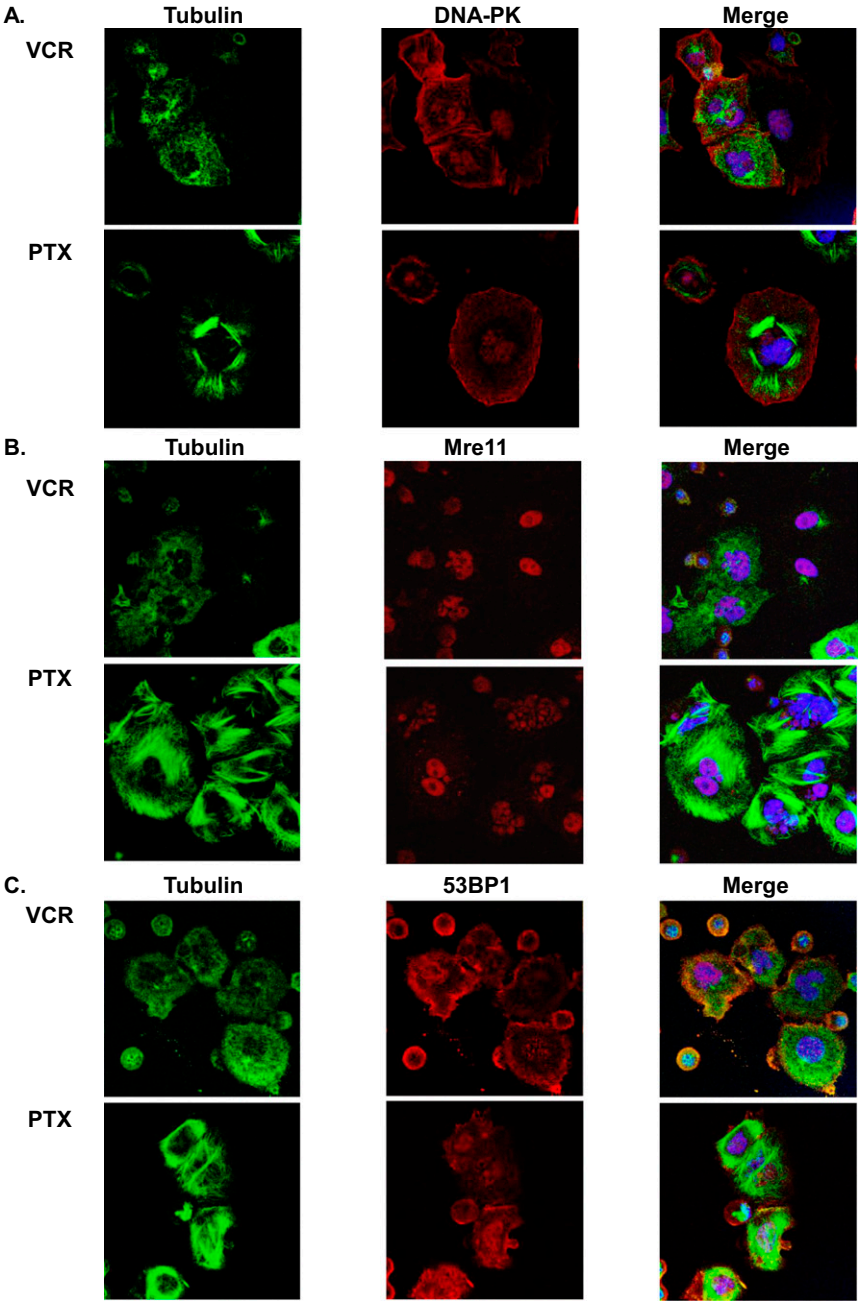

Fig. S2. (Continued)

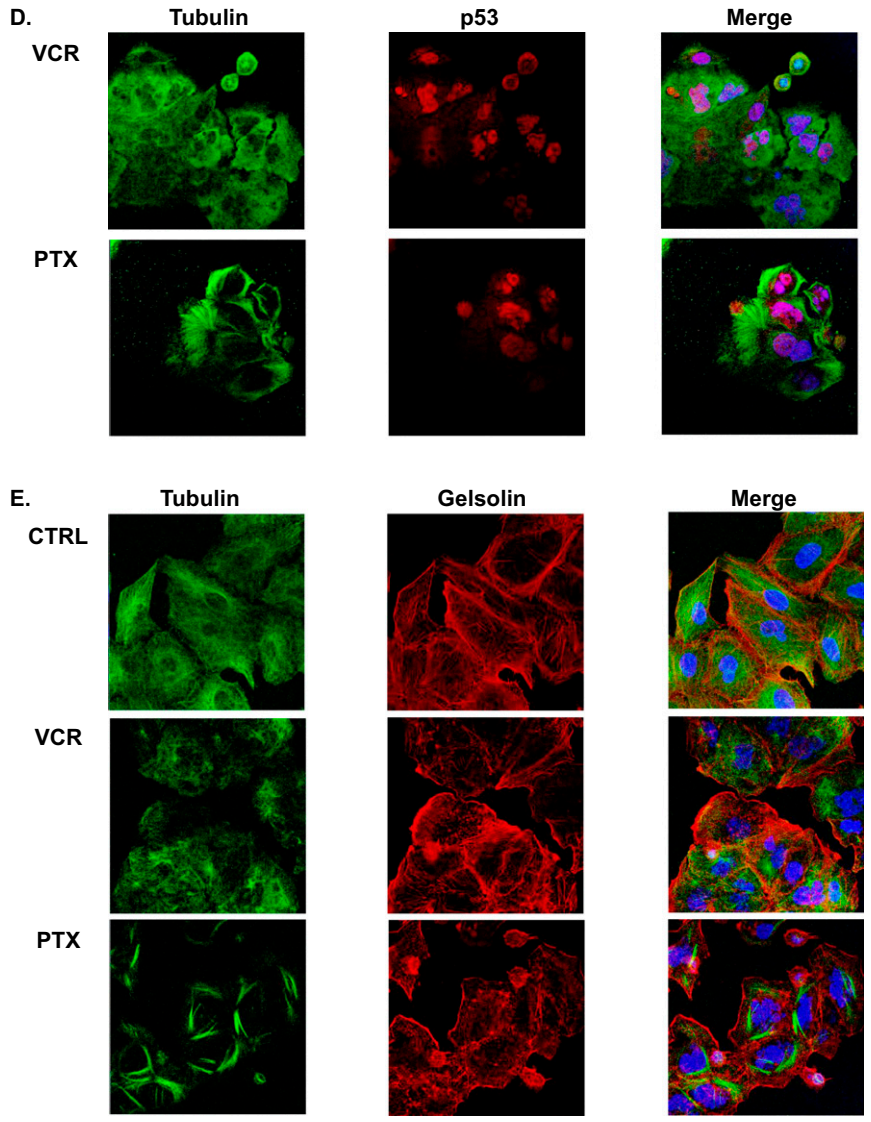

Fig. S2. DNA damage-repair proteins do not colocalize with MTs that have been disrupted by treatment with vincristine or paclitaxel as visualized by immunofluorescence microscopy. Confocal immunofluorescent localization of DNA damage-repair proteins. A549 cells treated with either 100 nM vincristine (VCR) or 200 nM paclitaxel (PTX) for 24 h were fixed and stained for tubulin and DNA-PK (*A*), Mre11 (*B*), 53BP1 (*C*), or p53 (*D*). Tubulin (FITC-conjugated secondary antibody, green); DNA repair proteins (RHOD-conjugated secondary antibody, red); DAPI (blue) localizes to cell nuclei. The tricolor localization of "Tubulin/DNA-damage-repair-protein/DAPI" is shown by the superimposition of three confocal images in the third column panels (Merge). Images are shown as 3D maximal projections reconstructed from *z*-stacks. Gelsolin, used as a control that neither binds tubulin nor accumulates in the nucleus, localizes to actin and the cytoplasm and does not colocalize with MTs nor accumulate in nuclei as visualized by confocal immunofluorescent microscopy. (*E*) A549 cells were either untreated (Ctrl) or treated with 100 nM vincristine (VCR) or 200 nM paclitaxel (PTX) for 24 h, fixed and stained with anti-tubulin (FITC-conjugated secondary antibody, green); and antigelsolin (RHOD-conjugated secondary antibody, red), then visualized using DAPI (blue) to identify nuclei. The tricolor localization of "Tubulin/Gelsolin/DAPI" is shown by the superimposition of three confocal images in the third column panels (Merge). Images are shown as 3D maximal projections reconstructed from *z*-stacks. (Magnification: 630×.)

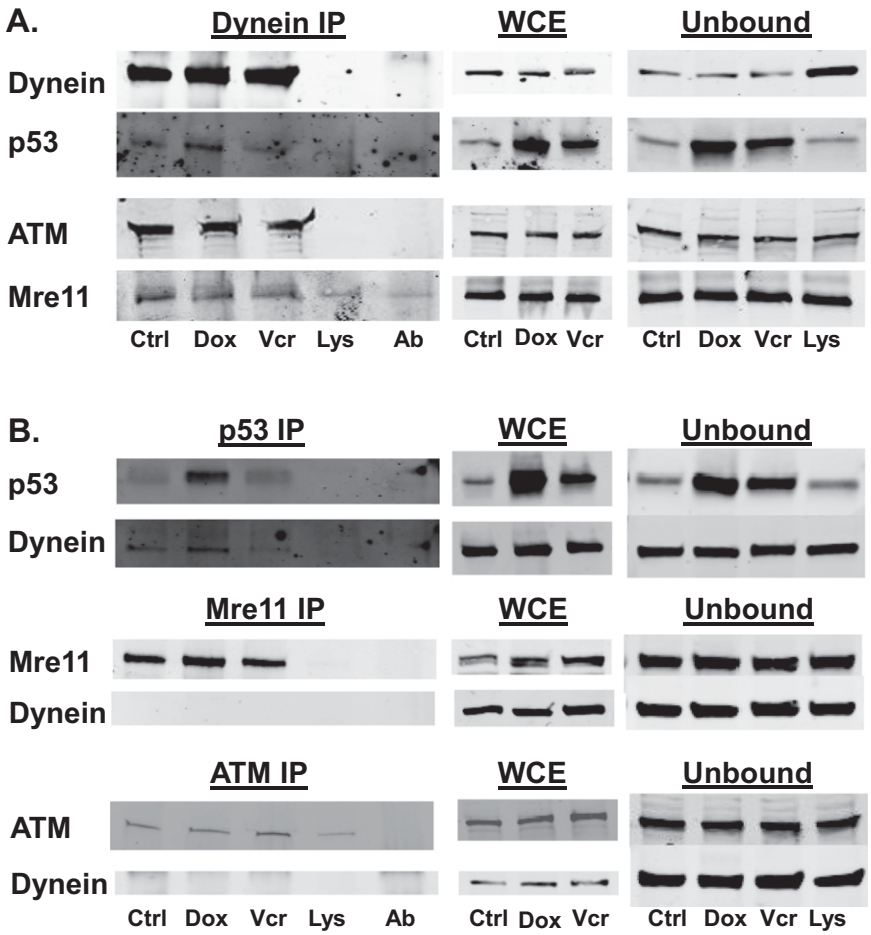

Fig. S3. Assessment of the depletion of proteins from supernatants following immunoprecipitations (IPs). IPs of A549 cell lysates from untreated cells (Ctrl), cells treated with 400 ng/mL doxorubicin for 4 h (Dox) or 100 nM vincristine for 20 h (Vcr) were immunoblotted as were two immunoprecipitation controls: lysate only (Lys, no immunoprecipitations performed) and IgG (Ab, control antibody). 50 μg of whole cell extract (WCE) and 30 μg of unbound immunoprecipitation samples (the supernatants) were immunoblotted for the same proteins. The protein loaded in the blots examining the immunoprecipitates represents all of that protein that was immunoprecipitated from 1 mg of cell lysate. (*A*) Dynein immunoprecipitations were immunoblotted for dynein, p53, ATM, and Mre11. Depletion of immunoprecipitation protein is observed in the unbound samples stained for dynein, but not for the other proteins. Apparent depletion in p53 in the first and last lanes is a reflection of the low levels of p53 in this cell line with a wild-type p53 and the higher levels achieved when cells are treated with doxorubicin or vincristine. (*B*) Depletion of the immunoprecipitated protein from unbound samples is not observed in the p53, Mre11, or ATM immunoprecipitations. In the p53 immunoprecipitation one can see some coimmunoprecipitation of dynein, but in the MRE11 and ATM, immunoprecipitations where only a small fraction of the total protein was immunoprecipitated, coprecipitation of dynein could not be detected.

Table S1. Treatment recommendations of approved combination chemotherapy including a DNA damaging and antimicrotubule agent in different malignancies

Disease	Regimen
Nonsmall cell lung cancer, metastatic	Cisplatin or carboplatin + Paclitaxel (1)
	Cisplatin or carboplatin + Docetaxel (2)
	Cisplatin or carboplatin + Vinorelbine (3)
Invasive breast cancer, neo-adjuvant/adjuvant	Cyclophosphamide + Docetaxel (4)
	Doxorubicin + Cyclophosphamide + Docetaxel (5)
	Carboplatin + Docetaxel + Trastuzumab (6)
Invasive breast cancer, metastatic or recurrent	Gemcitabine + Paclitaxel (7)
	Capecitabine + Docetaxel (8)
Ovarian cancer, adjuvant/advanced	Carboplatin + Paclitaxel (9)
	Carboplatin + Docetaxel (10)
Cervical cancer, metastatic or recurrent	Cisplatin + Paclitaxel (11)
Endometrial cancer, metastatic or recurrent	Carboplatin + Paclitaxel (12)
Bladder cancer, Neoadjuvant/metastatic	MVAC: Methotrexate + Vinblastine + Doxorubicin + Cisplatin (13)
Head and neck cancer, neoadjuvant	Cisplatin + Docetaxel + 5FU (14)
Head and neck cancer, metastatic or recurrent	Cisplatin or carboplatin + Docetaxel (15) Cisplatin or carboplatin + Paclitaxel (15)
Hodgkin lymphoma	ABVD: Doxorubicin + Bleomycin + Vinblastine + Dacarbazine (16)
Non-Hodgkin lymphoma, diffuse large B-cell lymphoma	RCHOP: Rituximab, Cyclophosphamide + Doxorubicin + Vincristine + Prednisone (17)
Non-Hodgkin lymphoma, indolent B-cell lymphoma	RCOP: Rituximab + Cyclophosphamide + Vincristine + Prednisone (18)
Occult primary, adenocarcinoma or squamous	Carboplatin + Paclitaxel + Etoposide (19)
Gastric cancer, metastatic	Cisplatin + Docetaxel + 5-FU (20)
Esophageal cancer, Neo-adjuvant plus radiation	Carboplatin + Paclitaxel (21)
Pheochromocytoma	Cyclophosphamide + Vincristine + Dacarbazine (22)

Summary tabulation of approved combination chemotherapy recommended regimens, which include both a DNA damaging and a MTA for a variety of malignancies.

1. Belani CP, et al. (2008) Randomized, phase III study of weekly paclitaxel in combination with carboplatin versus standard every-3-weeks administration of carboplatin and paclitaxel for patients with previously untreated advanced non-small-cell lung cancer. *J Clin Oncol* 26(3):468–473.
2. Fossella F, et al. (2003) Randomized, multinational, phase III study of docetaxel plus platinum combinations versus vinorelbine plus cisplatin for advanced non-small-cell lung cancer: The TAX 326 study group. *J Clin Oncol* 21(16):3016–3024.
3. Kelly K, et al. (2001) Randomized phase III trial of paclitaxel plus carboplatin versus vinorelbine plus cisplatin in the treatment of patients with advanced non–small-cell lung cancer: A Southwest Oncology Group trial. *J Clin Oncol* 19(13):3210–3218.
4. Jones S, et al. (2009) Docetaxel with cyclophosphamide is associated with an overall survival benefit compared with doxorubicin and cyclophosphamide: 7-year follow-up of US Oncology Research Trial 9735. *J Clin Oncol* 27(8):1177–1183.
5. Mackey JR, et al.; TRIO/BCIRG 001 investigators (2013) Adjuvant docetaxel, doxorubicin, and cyclophosphamide in node-positive breast cancer: 10-year follow-up of the phase 3 randomised BCIRG 001 trial. *Lancet Oncol* 14(1):72–80.
6. Sikov WM, et al. (2009) Frequent pathologic complete responses in aggressive stages II to III breast cancers with every-4-week carboplatin and weekly paclitaxel with or without trastuzumab: A Brown University Oncology Group Study. *J Clin Oncol* 27(28):4693–4700.
7. Albain KS, et al. (2008) Gemcitabine plus paclitaxel versus paclitaxel monotherapy in patients with metastatic breast cancer and prior anthracycline treatment. *J Clin Oncol* 26(24): 3950–3957.
8. O'Shaughnessy J, et al. (2002) Superior survival with capecitabine plus docetaxel combination therapy in anthracycline-pretreated patients with advanced breast cancer: Phase III trial results. *J Clin Oncol* 20(12):2812–2823.
9. Parmar MK, et al.; ICON and AGO Collaborators (2003) Paclitaxel plus platinum-based chemotherapy versus conventional platinum-based chemotherapy in women with relapsed ovarian cancer: The ICON4/AGO-OVAR-2.2 trial. *Lancet* 361(9375):2099–2106.
10. Vasey PA, et al.; Scottish Gynaecological Cancer Trials Group (2004) Phase III randomized trial of docetaxel-carboplatin versus paclitaxel-carboplatin as first-line chemotherapy for ovarian carcinoma. *J Natl Cancer Inst* 96(22):1682–1691.
11. Monk BJ, et al. (2009) Phase III trial of four cisplatin-containing doublet combinations in stage IVB, recurrent, or persistent cervical carcinoma: A Gynecologic Oncology Group study. *J Clin Oncol* 27(28):4649–4655.
12. Fleming GF, et al. (2004) Phase III trial of doxorubicin plus cisplatin with or without paclitaxel plus filgrastim in advanced endometrial carcinoma: A Gynecologic Oncology Group Study. *J Clin Oncol* 22(11):2159–2166.
13. Loehrer PJ, Sr, et al. (1992) A randomized comparison of cisplatin alone or in combination with methotrexate, vinblastine, and doxorubicin in patients with metastatic urothelial carcinoma: A cooperative group study. *J Clin Oncol* 10(7):1066–1073.
14. Vermorken JB, et al.; EORTC 24971/TAX 323 Study Group (2007) Cisplatin, fluorouracil, and docetaxel in unresectable head and neck cancer. *N Engl J Med* 357(17):1695–1704.
15. Stathopoulos GP, Rigatos S, Papakostas P, Fountzilas G (1997) Effectiveness of paclitaxel and carboplatin combination in heavily pretreated patients with head and neck cancers. *Eur J Cancer* 33(11):1780–1783.
16. Canellos GP, et al. (1992) Chemotherapy of advanced Hodgkin's disease with MOPP, ABVD, or MOPP alternating with ABVD. *N Engl J Med* 327(21):1478–1484.
17. Fisher RI, et al. (1993) Comparison of a standard regimen (CHOP) with three intensive chemotherapy regimens for advanced non-Hodgkin's lymphoma. *N Engl J Med* 328(14):1002–1006.
18. Marcus R, et al. (2005) CVP chemotherapy plus rituximab compared with CVP as first-line treatment for advanced follicular lymphoma. *Blood* 105(4):1417–1423.
19. Hainsworth JD, et al. (2010) Paclitaxel/carboplatin/etoposide versus gemcitabine/irinotecan in the first-line treatment of patients with carcinoma of unknown primary site: A randomized, phase III Sarah Cannon Oncology Research Consortium Trial. *Cancer J* 16(1):70–75.
20. Van Cutsem E, et al.; V325 Study Group (2006) Phase III study of docetaxel and cisplatin plus fluorouracil compared with cisplatin and fluorouracil as first-line therapy for advanced gastric cancer: A report of the V325 Study Group. *J Clin Oncol* 24(31):4991–4997.
21. van Hagen P, et al.; CROSS Group (2012) Preoperative chemoradiotherapy for esophageal or junctional cancer. *N Engl J Med* 366(22):2074–2084.
22. Averbuch SD, et al. (1988) Malignant pheochromocytoma: Effective treatment with a combination of cyclophosphamide, vincristine, and dacarbazine. *Ann Intern Med* 109(4):267–273.

Table S2. Proteomic analysis of dynein immunoprecipitates identifies additional DNA damage-repair protein candidates that might also traffic on MTs

Proteins	Description
Nuclear proteins involved in DNA repair and not studied in detail	
CETN2	Centrin, EF-hand protein, 2
DDB1	Damage-specific DNA binding protein 1, 127 kDa
ERCC5	Excision repair cross-complementing rodent repair deficiency, complementary group 5
MSH2	mutS homolog 2, colon cancer, nonpolyposis type 1
PCNA	Proliferating cell nuclear antigen
PMS1	PMS1 postmeiotic segregation increased 1
RAD52	RAD52 homolog
DDB1	Damage-specific DNA binding protein 1, 127 kDa
RAD51AP2	RAD51-associated protein 2
Additional nuclear proteins (peptides) also identified	
AURKB	Aurora kinase B (fragment)
BUB3	Mitotic checkpoint protein BUB3 (fragment)
HAT1	Isoform B of Histone acetyltransferase type B catalytic subunit
SAP18	Histone deacetylase complex subunit SAP18
SAP30BP	SAP30-binding protein
H3F3A	Histone H3
HIST2H3PS2	Histone H3
HIST1H2BL	Histone H2B type 1-L
HIST1H2AC	Histone H2A type 1-C
HIST2H2AC	Histone H2A type 2-C
H1F0	Isoform 2 of Histone H1.0
HIST1H2AJ	Histone H2A type 1-J
HIST1H1C	Histone H1.2
HIST1H4A	Histone H4
Additional proteins (peptides) of interest	
RRAS	Ras-related protein R-Ras
RRAS2	Isoform 2 of Ras-related protein R-Ras2
RASEF	Ras and EF-hand domain-containing protein
RAB10	Ras-related protein Rab-10
RAB1B	Ras-related protein Rab-1B
RAB6B	Ras-related protein Rab-6B (Fragment)
RAB13	Ras-related protein Rab-13
RAB14	Ras-related protein Rab-14
RAB18	Ras-related protein Rab-18
RHOC	Ras homolog gene family, member C (fragment)
Multiple	29 mitochondrial and mitochondria-associated proteins